Harmonic Iron Losses in Stator Core of Brushless Motor with Various Electrical Steels

[1]K. H. Ha, [1]S. Y. Cha, [1]J. K. Kim, [2]Y. Hur, [2]Y. S. Lim, and [3]J. P. Hong, Senior Member, *IEEE*

[1]Electrical Steel Research Group, Technical Research Laboratories, POSCO
#1, Goedongdong, Namgu, Pohang, Gyeongbuk, Korea, phone: (+8254)2206164, fax: (+8254) 2206913
[2]R&D PCM Team, Techical Center, Daewoo Presision Industries Co. Ltd., Korea
[3]Department of Electrical Engineering, Changwon National University, Korea
e-mail: khha@posco.co.kr, yslim@dpi.daewoo.co.kr, jphong@sarim.changwon.ac.kr

Abstract — **This paper investigates the iron losses and their behavior in the stator core for various electrical steels considering the complex flux waveform and the variable flux density. The elliptical rotating and alternating flux distributions with non-sinusoidal waveforms are analyzed by Finite Element Method (FEM) and then their harmonic components are extracted. Based on these results, the distribution of local iron losses in the stator core caused by the harmonic flux is calculated. The iron loss in the motor running are investigated by using the various non-oriented electrical steels for stator core that have different magnetic properties at high frequencies.**

I. INTRODUCTION

The high efficiency for motors has been continuously required for energy saving. The optimal utilization related to the machine design and manufacturing process is used for the reduction of losses. The iron losses occurring in motor cores account for high percentage in the energy losses of motors, so that electrical steels with lower iron losses have been desired. The electrical engineers have predicted the iron loss in rotating machines by using Epstein test measured under the alternating flux excitation in the core. However, the flux patterns in the motor core are very complex [1-3]. The complex magnetizing condition is supposed to occur locally, such as the flux waveform distortion and the rotation magnetization. These phenomena in the stator core depend on the operating conditions, input source, and machine structures, which lead to the increase in iron losses. It is therefore important to understand the flux distribution within the core and the iron loss behavior due to harmonic field components. The comprehensive understanding iron loss behavior helps to design the high efficiency motor, and select the analysis method and the material data considering the actual magnetic field in the core.

A standard method of analyzing the iron loss is to break it up to static hysteresis loss, classical eddy current loss and anomalous loss due to domain wall effects. To obtain reliable estimates of the iron loss, it is important to determine formula to evaluate loss, magnetic flux density used for iron loss calculation and the magnetic property data of materials used in loss calculation. For the formula, the various physical models have been proposed. One of many equations is as follows [2]:

$$P_c = k_h f B^n + k_e f^2 B^2 + k_a f^{1.5} B^{1.5} \tag{1}$$

Then flux density distribution obtained by magnetic field analysis. The use of magnetic property data is classified into three groups: the experimental loss constant coefficient, the loss data base versus flux density or frequency, and hysteresis and eddy current loss data extracted from the loss data base. We have proposed the iron loss analysis method and proved the validation [3]. The iron loss is predicted using a numeric method for flux density and the iron loss curves tested on Epstein method. The losses were obtained by decomposing the flux in each element into its time harmonic components.

This paper describes the flux density behavior at local positions of the stator core and analyzes their harmonic iron loss distribution due to non-sinusoidal waveforms. The iron loss of a brushless motor is investigated using the various non-oriented electrical steels for stator core. The influence of various materials on the loss distribution is examined according to variable speed. As the analysis method mentioned above, it is selected that the finite element method used for the magnetic flux density distribution and the loss data measured by using ring specimen.

II. ANALYSIS MODEL AND METHOD

A. Analysis Model and Materials

Fig. 1 shows the analysis model that is an interior permanent magnet type brushless motor with four poles. The stator lamination is 70mm with 0.5(mm) silicon sheet steel. Tables I shows the magnetic properties for various electrical steels measured by using ring specimens at 60, 400 and 3000 (Hz). The A-type material is a high grade and the E-type material is the lowest magnetic properties in the five grades. In the Epstein test, the magnetic flux in the steel shared into 30×280mm strip pass through only two directions, rolling and transverse of electrical steel sheet. The various degrees of flux density polarization are encountered in rotating machines. Therefore, in this study, the iron loss data measured by using the ring shared into toroidal shape with 45mm outer diameter.

Fig. 2 shows the iron loss for A-Grade material at 60(Hz) according to the measuring method. The iron loss by the ring specimen is a considerable increase in the high flux density. This is due to the anisotropic depending on the magnetization direction in the non-oriented electrical steel material.

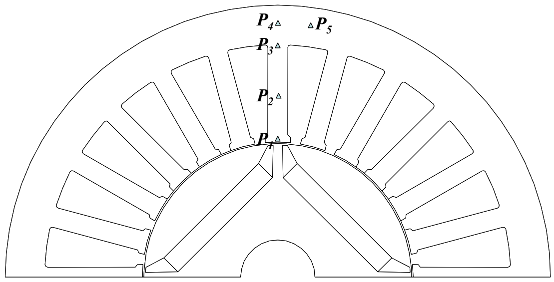

Figure 1. Brushless motor structure and observed points to evaluate flux behavior.

TABLE I IRON LOSS FOR VARIOUS MATERIALS MEASURED BY RING SAMPLES
($W_{A/B}$: IRON LOSS FOR A×0.1 FLUX DENSITY AT B FREQUENCY)

	A-Grade	B-Grade	C-Grade	D-Grade	E-Grade
$W_{15/60}$ (W/kg)	5.57	6.37	7.85	8.42	9.28
$W_{10/400}$ (W/kg)	27.24	31.22	40.55	42.84	57.88
$W_{10/3000}$ (W/kg)	952.9	1082.0	1398.5	1513.5	2150.0

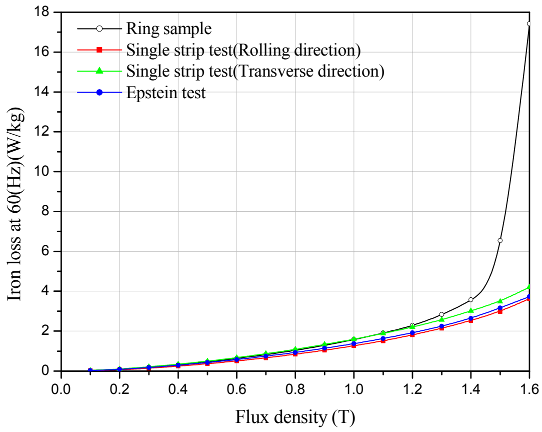

Figure 2. Measured iron loss data of B-Grade material for various samples.

B. Analysis Method

The temporal and the spatial variations of the magnetic flux density waveforms are derived by performing 2-Dimensional Finite Element Method (2-D FEM). The governing equation for solving the brushless motor with the permanent magnet from Maxwell's electromagnetic equation is as follows:

$$\nabla \times (\frac{1}{\mu} \nabla \times \vec{A}) = \vec{J}_0 + \vec{J}_m \tag{2}$$

where μ is the magnetic permeability, A is the magnetic vector potential, J_o is the current density and J_m is the magnetization of permanent magnet.

Discrete Fourier Transform (DFT) is used for the frequency analysis of the time-varying magnetic flux density waveforms at each element of the finite element analysis model. DFT can be expressed as:

$$B_k(k) = \sum_{n=0}^{N-1} B_p(n) e^{j(2\pi nk)/N} \tag{3}$$

where k is the harmonic order, N is the number of the discrete data, $B_k(k)$ is the peak value of the magnetic flux density of the k^{th} harmonic, and $B_p(n)$ is the magnitude of the point n.

The iron losses resulting from the flux density harmonic components at each element are found from the interpolation of the measured loss data points. The cubic-spline is used for data in two-dimensional function table. The iron loss summation to N^{th} harmonic component in an element is as follows.

$$w_e = \sum_{k=1}^{N} w(B_k, f_k) \tag{4}$$

where w_e is the iron loss at an element, and w is the iron data of electrical steels as a function of frequency and flux density.

Finally, the total iron loss is obtained by the summation of the iron losse in all the elements.

$$W_t = \sum_{m=1}^{Nele} w_e \tag{5}$$

where W_t is the total iron loss of analysis model, and N_{ele} is the number of element.

III. ANALYSIS RESULTS AND DISCUSSION

A. Flux Density Distribution

Fig. 3 shows the loci of flux density at the five positions in the stator core as shown in Fig. 1. The observing points are tooth tip, tooth body, tooth root, and two different positions on the yoke. These results are obtained from the magnetic field analysis under the excitation of permanent magnet. In the tooth part, the tooth body P2 has considerable the normal components compared to P1 and P3. In the yoke part, the tangential component is comparable to the normal flux in P4 and P5. As a result, the flux variation is nearly circular at the teeth roots and elliptical at the tooth tips. Then the local flux density in the teeth body and yokes has the alternating flux. The distortion factor for the flux density is calculated to evaluate the non-sinusoidal characteristic of flux wave. The distortion factor in the teeth parts is about 3%, and that in the yoke part is less than 1%.

The axis ratio β is defined as the maximum value to the minimum value in the loci of flux density ($\beta = B_{min}/B_{max}$). We assume that the alternating flux is β<0.1 and the rotating flux is β>0.1. Fig. 4 shows the coloring and contour of axis ratio of the flux density loci in the stator core. The alternating flux region is present along the yoke and the teeth body, displayed as arrows on the stator core. The rotating flux region is displayed on the teeth root and the teeth tip. The area with the rotating flux is about 70% to the stator core.

B. Iron Loss Behavior

Fig. 5 shows the iron loss density distribution and the harmonic loss distribution due to the harmonic flux density except for the fundamental component. The fundamental frequency is 100(Hz). There is a considerable high loss region at the teeth root and tip region because of the rotating flux, as shown in Fig. 5(b). The loss distributions are similar to the axis ratio distribution of flux density waveform in Fig. 4.

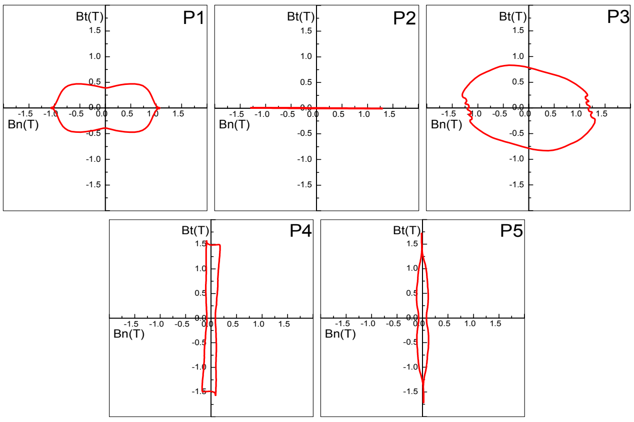

Figure 3. Loci of flux density at five different positions in stator core.

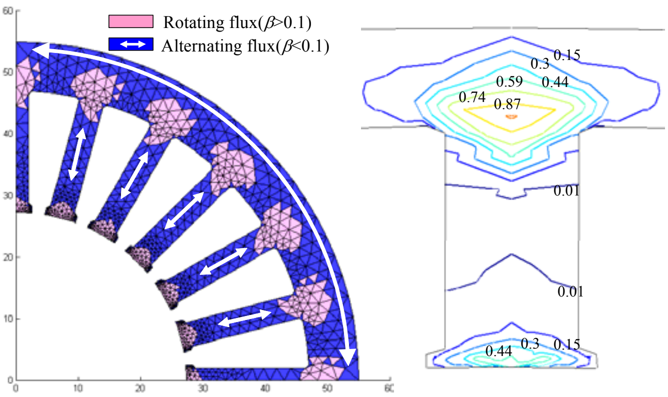

Figure 4. Coloring and contour of axis ratio of flux density waveform in stator core.($\beta = B_{min}/B_{max}$)

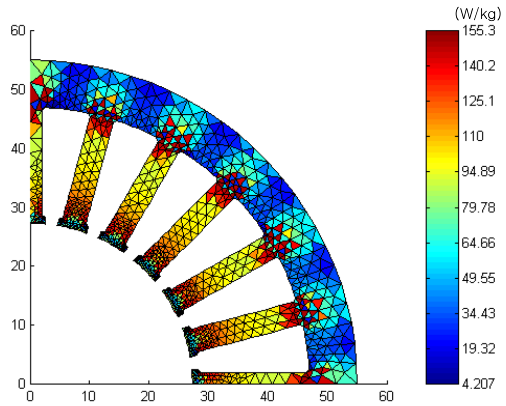

(a) Total iron loss

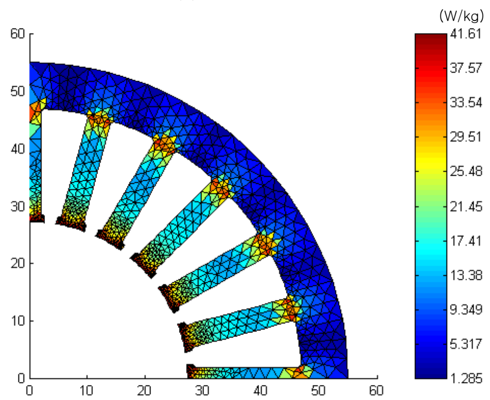

(b) Harmonic loss due to harmonic components of flux density

Figure 5. Iron loss density distribution.

The rotating field has influence on the increase of iron loss. Fig. 6 shows the loss analysis results for each order of the flux density and the sum of harmonic loss up to 50th order. The harmonic iron loss grows steadily and then remains almost constant at 50th order.

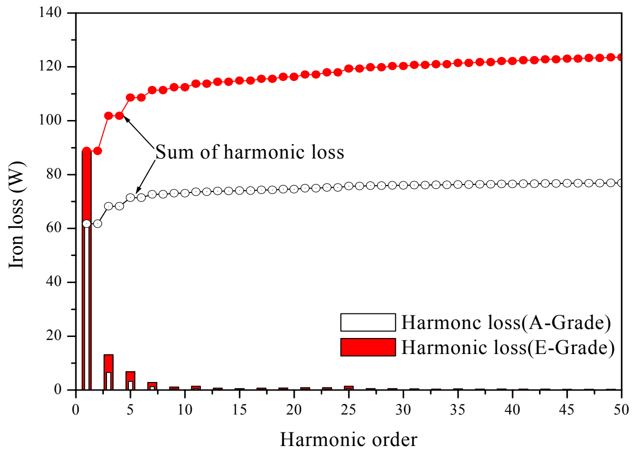

Figure 6. Harmonic loss analysis results for each components and the sum of harmonic loss up to 50th order with A-Grade and E-Grade materials.

C. Various Materials

The effects of various materials on the iron loss are investigated. Table II presents the iron loss in the stator for various materials. From the results of E-Grade material, the total iron loss to the 50th harmonic component are 123.5(W), and the iron loss except for the fundamental component is 34.8(W) occupying about 28.1% in the total iron loss. Therefore, it is very important to analyze the iron loss considering the harmonic components in the alternating and rotating field. The harmonic loss decreases in the high grade material. The high grade A-type material reduces the iron loss about 60.6% compared to the low grade E type material.

Fig. 7 shows the iron loss varying with the speed of motor with various electrical steel materials. Fig. 8 shows the iron loss due to the fundamental component and the harmonic component versus motor speed. The iron loss is affected by the motor speed. Fig. 9 presents the iron loss curve versus flux density of A-Grade material measured by using ring specimens at from 50(Hz) to 15(kHz). To find the iron loss for the harmonic flux density and its frequency, the raw material data set is interpolated as plotted on the Fig. 9

Fig. 10 shows the iron loss resulting from the alternating and rotating flux pattern with various materials. The iron loss caused by the rotating flux is about 70% to the total iron loss. Fig. 11 shows the equipotential line of analysis model.

TABLE II IRON LOSS IN THE STATOR FOR VARIOUS MATERIALS (W_T: TOTAL IRON LOSS, W_H: HARMONIC LOSS, ΔW: IMPROVEMENT FOR A-GRADE)

	A-Grade	B-Grade	C-Grade	D-Grade	E-Grade
W_t (W)	76.9	84.0	100.6	110.8	123.5
W_h (W)	15.2	17.8	27.8	32.6	34.8
W_h/W_t (%)	19.7	21.2	27.6	29.4	28.1
ΔW (%)	-	9.2	30.8	44.1	60.6

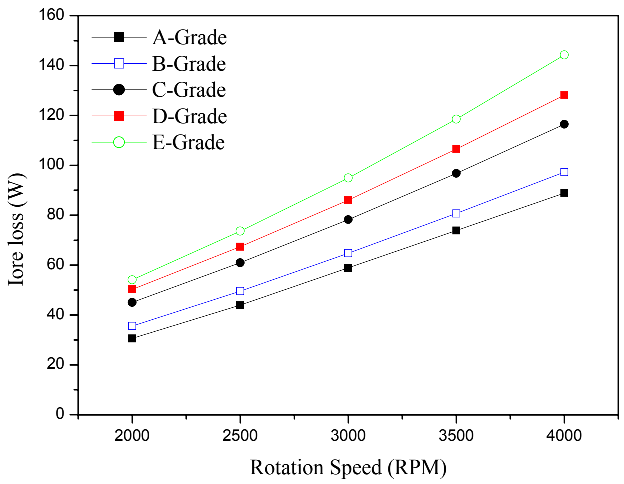

Figure 7. Iron loss versus speed of motor with various electrical steel materials.

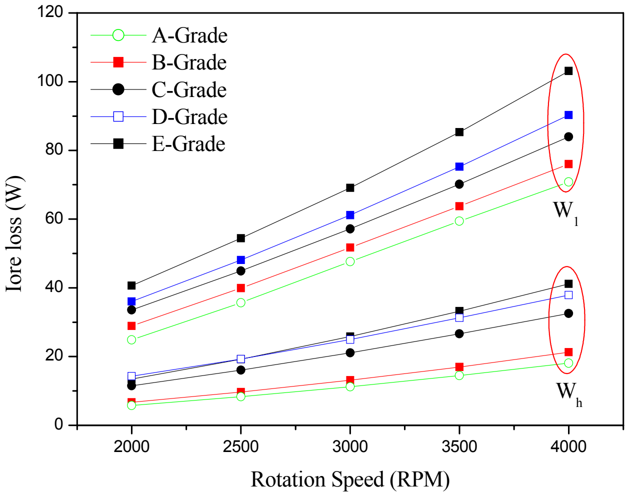

Figure 8. Iron loss due to fundamental component and harmonic component versus rotation speed of motor with various electrical steel materials.

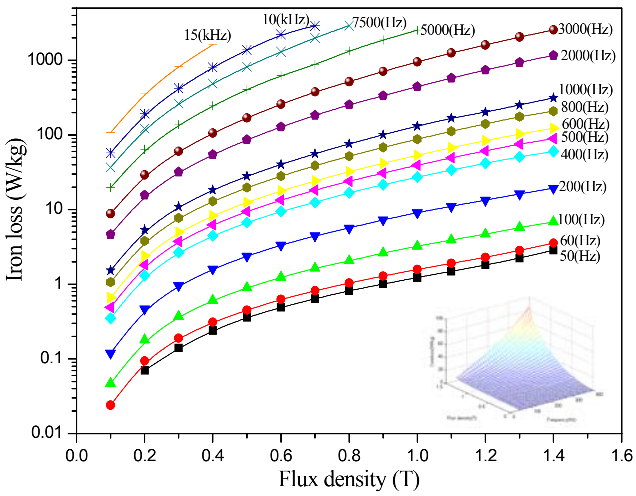

Figure 9. Iron loss curve versus flux density of A-Grade material measured by using ring samples at from 50(Hz) to 15(kHz).

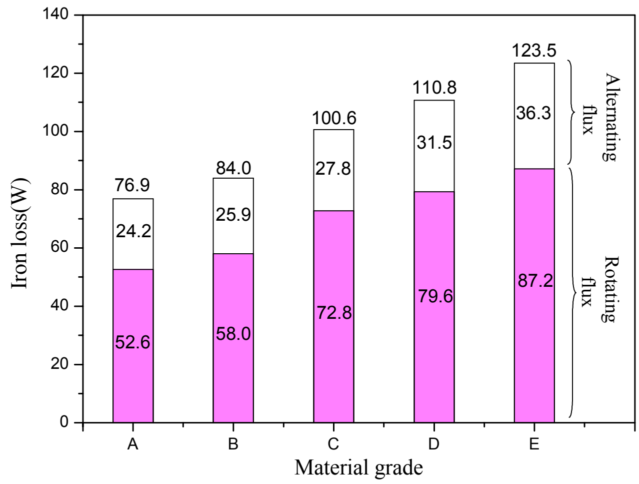

Figure 10. The iron loss due to the rotating and alternating flux.

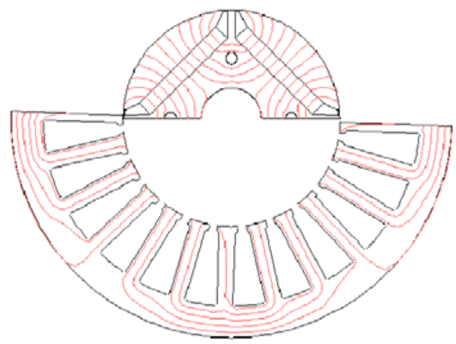
Figure 11. Equipotential distribution of analysis model.

IV. Conclusions

This paper presents the flux density distribution and the iron loss due to the non-sinusoidal flux wave in the stator core. The brushless motors with the various non-oriented electrical steels are used. The flux variation is nearly circular at the teeth root and the teeth tip. Then the flux density in the teeth body and yoke has the alternating flux. The loci, axis ratio, iron loss and distortion factor of flux density is used for accessing the flux distribution. The effects of various materials on the iron loss are investigated. The harmonic iron loss is occupying about 28.1% to the total iron loss in the low grade material. The high grade material reduces the iron loss about 60.6% compared to the low grade material.

V. References

[1] J. G. Zhu and Victor Stuart Ransden, "Improved Formulations for Rotational Core Losses in Rotating electrical Machines," *IEEE Tans. on Magn.* Vol. 34, No. 4, pp. 2234-2242, 1998.

[2] Y. Chen and P. Pillay, "An Improved Formula for Lamination Core Loss Calculations in Machines Operating with High Frequency and High Flux Density Excitation," *Proceeding of IEEE-IAS'2002, Pittsburg, USA*, Vol. 2, pp. 759 – 766, 2002.

[3] H. Nam, K. H. HA, J. J. Lee and J. P. Hong, "A Study on Iron Loss Analysis Method Considering the Harmonics of the Flux Density Waveform using Iron Loss Curves Tested on Epstein Samples," *IEEE Trans. on Magn.,* Vol. 39, No. 3, pp. 14721475, 2003.